Simultaneous tracking of 3D actin and microtubule strains in individual MLO-Y4 osteocytes under oscillatory flow

Andrew D. Baik [a], Jun Qiu [b], Elizabeth M.C. Hillman [c], Cheng Dong [d], X. Edward Guo [a,*]

[a] Bone Bioengineering Laboratory, Department of Biomedical Engineering, Columbia University, NY, USA
[b] School of Aerospace, Tsinghua University, Beijing, PR China
[c] Laboratory for Functional Optical Imaging, Department of Biomedical Engineering, Columbia University, NY, USA
[d] Department of Bioengineering, Pennsylvania State University, University Park, PA, USA

ABSTRACT

Osteocytes *in vivo* experience complex fluid shear flow patterns to activate mechanotransduction pathways. The actin and microtubule (MT) cytoskeletons have been shown to play an important role in the osteocyte's biochemical response to fluid shear loading. The dynamic nature of physiologically relevant fluid flow profiles (*i.e.*, 1 Hz oscillatory flow) impedes the ability to image and study both actin and MT cytoskeletons simultaneously in the same cell with high spatiotemporal resolution. To overcome these limitations, a multi-channel quasi-3D microscopy technique was developed to track the actin and MT networks simultaneously under steady and oscillatory flow. Cells displayed high intercellular variability and intracellular cytoskeletal variability in strain profiles. Shear E_{xz} was the predominant strain in both steady and oscillatory flows in the form of viscoelastic creep and elastic oscillations, respectively. Dramatic differences were seen in oscillatory flow, however. The actin strains displayed an oscillatory strain profile more often than the MT networks in all the strains tested and had a higher peak-to-trough strain magnitude. Taken together, the actin networks are the more responsive cytoskeletal networks in osteocytes under oscillatory flow and may play a bigger role in mechanotransduction pathway activation and regulation.

1. Introduction

Osteocytes have been hypothesized as mechanosensors in bone that can directly regulate bone turnover and adaptation [1]. Mechanical load-induced oscillatory fluid flow through the lacun-canalicular system has been proposed to induce shear stresses over the cell body and processes of osteocytes in the pericellular space to activate biochemical pathways [2,3]. Most *in vitro* cell studies of osteocytes under oscillating flow have been performed on confluent, adherent osteocytes. Very few studies have considered the mechanical behavior of osteocytes at the single cell level [4–6]. However, osteoblasts are morphologically and biochemically distinct from osteocytes [7]. This highlights the need to characterize osteocyte mechanics under a range of physiologically relevant fluid shear flow patterns.

Previous *in vitro* fluid shear studies on primary osteocytes and osteocyte cell lines have focused on flat, spread osteocytes, but the *in vivo* cell body shape of osteocytes is ellipsoidal or spherical

[8,9]. Osteocytes in this 3D configuration have different mechanical properties and biochemical responses than when flat and spread [10]. Additionally, the actin and microtubule networks in round osteocytes are distributed differently than in spread osteocytes [11,12]. Downstream cytoskeletal remodeling events in osteocytes were also affected by the usage of oscillatory flow versus steady flow [13,14]. A previous study in our laboratory studied how actin and microtubule networks deformed individually in osteocytes, but a high degree of intercellular variability was seen [5]. Mechanical comparisons between the two networks were limited due to this heterogeneity between individual cells. Studies in actin and MT polymer gel solutions have revealed composite-like behavior when the two networks interact under mechanical loading [15,16]. Therefore, it was of interest in this study to characterize the deformational behavior of the actin and MT networks simultaneously in an osteocytes' cell body under a physiological level of fluid shear flow at the single cell level.

Limitations in temporal resolution of traditional raster-scanning 3D microscopy techniques (*i.e.*, confocal or deconvolution) have hindered the ability to capture the 3D mechanical behavior of osteocytes because of the dynamic nature of oscillating flow (1 Hz) and the near-instantaneous mechanical responses of the cell. We developed a "quasi-3D" microscopy technique that was

* Corresponding author. Address: Department of Biomedical Engineering, Columbia University, 351 Engineering Terrace, Mail Code 8904, 1210 Amsterdam Avenue, NY 10027, USA. Fax: +1 212 854 8725.

E-mail address: ed.guo@columbia.edu (X.E. Guo).

able to image a single cell in two orthogonal planes simultaneously while maintaining a high temporal resolution [5]. This technique allowed better spatiotemporal visualization of the dynamics of cellular deformation in 3D that would have been lost in the slower raster scanning techniques.

The viscoelastic deformational behavior between steady and oscillatory flow patterns in osteocytes will be compared using the actin and microtubule networks as measures of strain. By tracking both networks simultaneously using new developments in the quasi-3D microscopy technique, direct comparisons can now be made between the two networks, since the cytoskeletal analyses are paired and at a high enough temporal resolution to fully map out the oscillatory and steady loading profiles. The objectives of this study were to (1) simultaneously image in quasi-3D the actin and MT networks in osteocytes under steady and oscillatory fluid flow, (2) calculate the developed strains in the actin and MT networks under the different flow profiles, and (3) compare their behaviors within the same cell.

2. Methods

2.1. Quasi-3D microscopy

The basic quasi-3D design is presented in a previous study from our laboratory [5]. In brief, an inverted microscope and an upright microscope with a 45° mirror in its lightpath are focused on a single cell in a rectangular tube with 60× objectives (Fig. 1A). These microscopes are independently yet simultaneously focused on two orthogonal planes of the same cell, dubbed "bottom-view" and "side-view." For this current study, an additional functionality of simultaneous collection of up to four emission channels was added into the quasi-3D system. Two Quadview beamsplitters (Photometrics, Tucson, AZ) and custom-designed dichroics and excitation filters were used to visualize both the actin and microtubule networks simultaneously in quasi-3D. The multichannel quasi-3D system was designed to collect the emissions of the

following common dyes: CFP, YFP, mCherry/mkate2, and DiR (emission filters of 470/28, 530/30, 641/75, and 809/81, respectively) (Semrock, Rochester, NY). To achieve simultaneous dye excitation, a multi-band excitation filter was added to the xenon lamp light source to excite CFP and mkate2 (430/25 and 570/40). A custom-made dichroic was placed in the microscopes to reflect the excitation bands and pass-through the emission bands to the beamsplitter. DU-885 EMCCD cameras (Andor, Belfast, Northern Ireland) on each of the microscopes captured the bottom- and side-view emissions.

2.2. Cell culture

MLO-Y4 osteocyte-like cells (a gift from Dr. Lynda Bonewald of the University of Missouri-Kansas City) were grown in α-modified Eagle's medium supplemented with 5% fetal bovine serum and 5% calf serum. The Lifeact live-cell F-actin probe [17] was cloned into a TagCFP fusion plasmid (Evrogen, Moscow, Russia) to allow visualization of F-actin dynamics in cyan. The EMTB (ensconsin microtubule binding domain) MT probe [18] was cloned into an mkate2 fusion plasmid to allow visualization of MT dynamics in red/far-red. The TagCFP and mkate2 fluorescent protein variants were chosen to minimize spectral bleed-through of the fluorophores to negligible levels during simultaneous acquisition. Cells were double-transfected with the TagCFP-Lifeact and mkate2-EMTB plasmids 24 h prior to flow experiments using Fugene 6 (Roche Applied Science, Indiana, IN) according to manufacturer's instructions.

2.3. Fluid flow experiments

Twenty four hours after transfection, cells were trypsinized and plated on narrow glass slides for 45 min to ensure a fully attached, rounded cell shape. The glass slides were then placed into a square glass tube for imaging and flow. Hank's Buffered Saline Solution was used as flow media. Steady, unidirectional fluid flow ($n = 8$) at a wall shear stress of 10 dynes/cm^2 was achieved by using a
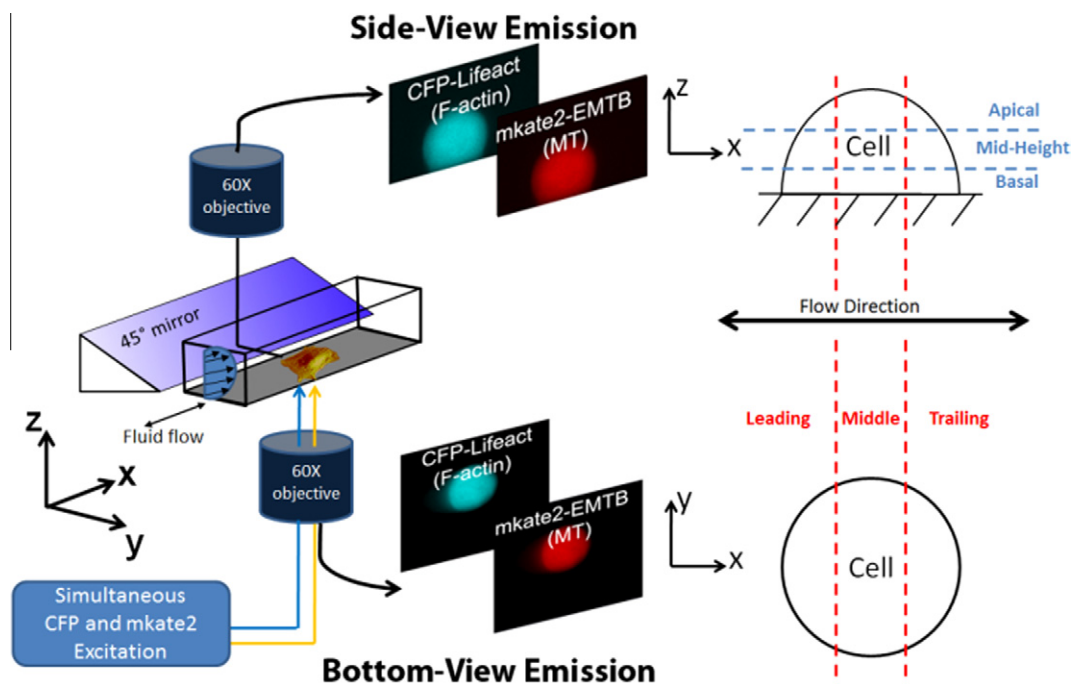
Fig. 1. Schematic of the multi-channel quasi-3D microscopy technique to visualize the F-actin and MT networks simultaneously. The CFP and mkate2 fluorophores are excited with a dual-excitation filter. A beamsplitter in both microscopes separates the CFP and mkate2 emissions. Each microscope's camera is synchronized to obtain images at the same timepoint. Definitions for subcellular regions in the two views are presented on the right.

syringe pump (New Era Pump Systems, Wantagh, NY) and gas-tight syringe (Hamilton, Reno, NV).

Dynamic, oscillatory fluid flow ($n = 7$) with a peak shear stress of 10 dynes/cm^2 was provided by a custom-built oscillatory pump [19]. The flow profile was sinusoidal at a 1 Hz frequency. Both flow types were applied to the flow chamber for 10 s. An individual cell was imaged in quasi-3D at a 10 Hz frequency to fully map out the fluid flow profiles.

2.4. Image analysis

All calculations were performed in MATLAB 7.8 (The Math-Works, Natick, MA). Intracellular displacement fields of the actin and MT networks for each cell were obtained identically for both bottom and side views according to a previously elaborated technique involving digital image correlation [5,20,21]. Displacement fields were first smoothed with a bilinear least squares filter [22] and then smoothed and differentiated using a thin-plate spline algorithm [23]. Finite Lagrangian strain fields were then calculated (three bottom-view strains: Eyy, bottom-view Exx, and Exy; and three side-view strains: Ezz, side-view Exx, and Exz). The absolute strain error on simulated rigid-body displacement actin and MT networks was 0.027 ± 0.0312 (%).

2.5. Strain analysis

Strains were averaged in various subcellular regions (Fig. 1B). For steady flow, exponential constants for strains that displayed
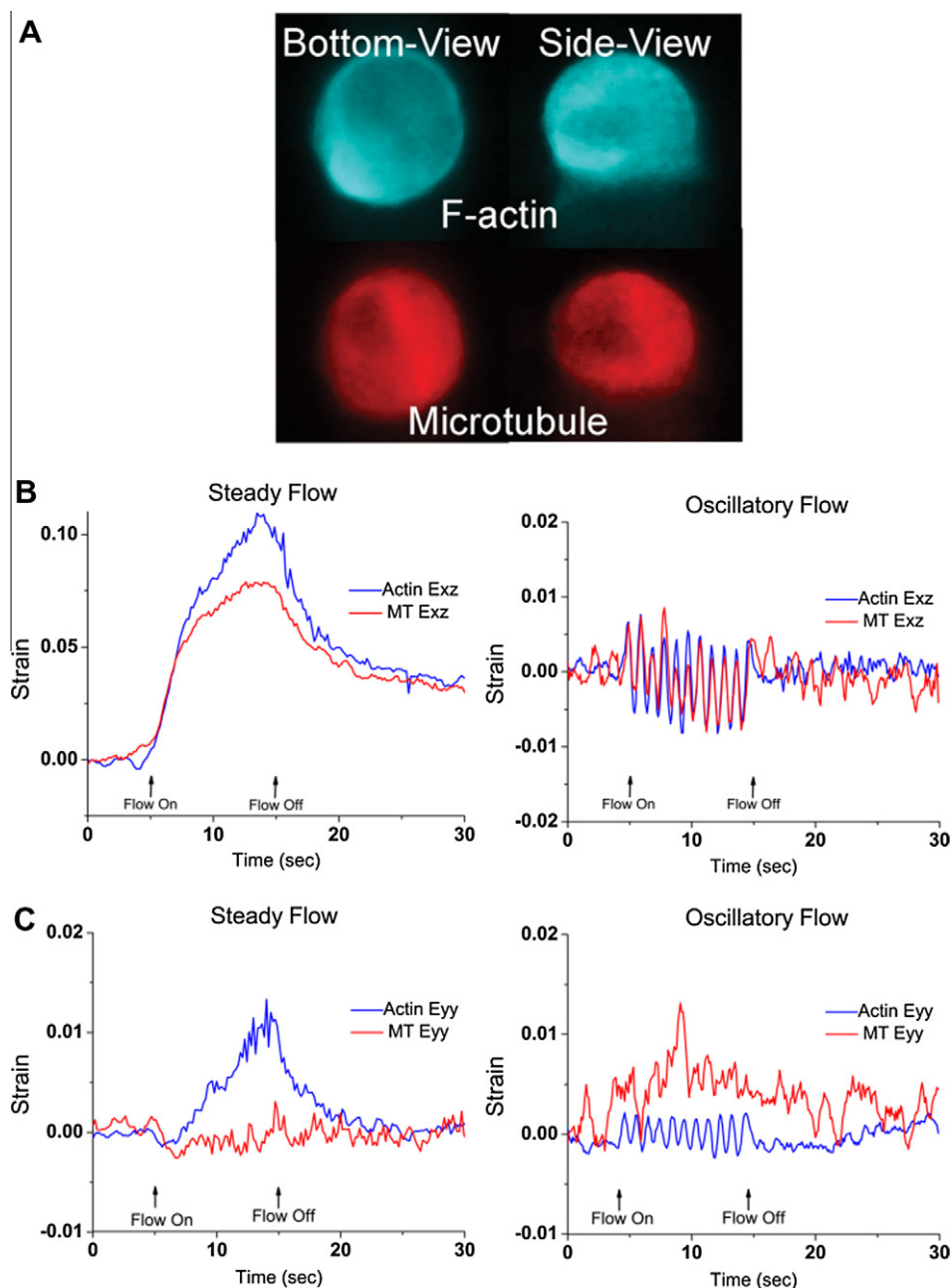
Fig. 2. (A) Sample image of the F-actin and microtubule networks of an MLO-Y4 osteocyte imaged simultaneously in two orthogonal planes (bottom and side views). (B) Sample side-view whole-cell shear Exz strain trace for both cytoskeletons under steady flow or oscillatory flow. Both networks display creep and creep-recovery behaviors in steady flow. Both networks display sinusoidal shear strains that follow the oscillatory flow pattern. (C) Sample side-view whole-cell shear Eyy strain trace for both cytoskeletons of a single osteocyte under steady or oscillatory flow that show different mechanical responses within the same cells between the two cytoskeletons. In these examples, only the actin network displays characteristic creep or oscillation.

creep and creep recovery behavior were extracted from strain time course plots. Strain time course plots for each region were fit to an exponential function $\varepsilon(t) = a + be^{-ct}$ using least squares curve fitting. Plots that converged were considered to have creep-like behavior and the exponential constants were used in further analyses. Strains that displayed creep-like behavior in both networks were directly compared in paired statistical tests.

Strain time course plots in oscillatory flow were run through a high pass filter, and plots that displayed periodic ~1 Hz behavior had the peaks and troughs extracted for further analyses.

2.6. Statistical analysis

All statistical analyses were performed using NCSS 2007 software (NCSS LLC, Kaysville, UT). Strain values for the actin and MT networks within each cell at different times or in subcellular regions were compared in paired analyses within a cell. Most comparisons were determined to have non-normal distributions, so the non-parametric Wilcoxon-signed rank test was used. The significance level, α, was set at 0.05.

3. Results

3.1. Simultaneous tracking of actin and MT networks under fluid flow

Using the dual-excitation filter and emission beamsplitter, the actin and microtubule networks in a single osteocyte were able to be imaged simultaneously (Fig. 2A). F-actin networks formed primarily cortical networks near the membrane with diffuse staining perinuclearly. MT networks were also perinuclear but were noticeably less prevalent near the plasma membrane. Both networks were excluded from the cell nucleus. F-actin was also visible in very short filopodia-like cellular processes in the basal periphery of the cell, given the short plating time. MT networks were not visible in this area. A high temporal resolution of 10 Hz was maintained, allowing instantaneous strain deformations, i.e., at the onset of flow, to be measured in steady and oscillatory fluid flow profiles (Fig. 2B and C).

3.2. Steady flow strain comparisons

Actin and MT networks tended to behave with viscoelastic creep and creep-recovery behaviors in the actin and MT networks strains under steady flow, confirming previous results [5]. This behavior was observed in 65.6% of the subcellular shear Exz in both networks but was also present to a lesser degree in the normal Ezz and Exx strains at 50.5% of the time. Bottom-view Eyy exhibited creep behavior only 27.1% of the time. There was no statistically significant difference in the occurring frequency of creep behavior between the two networks. However, some cells displayed creep behavior in only one of the networks and not the other.

Additionally, high variability was seen in the heterogeneous distribution of the strains of the actin and MT networks within the same cell (Fig. 3A). Peak strains at the end of the flow period were averaged in the subcellular regions of the cell (Fig. 3B and C). All comparisons were performed using paired statistical tests between the actin and MT networks within each cell. In the apical region, MT Exz was higher than actin Exz ($p < 0.01$) by an average of .0192. However, this difference was reversed in the basal region of the cell. Actin Exz was higher than MT Exz ($p < 0.05$) by an average of 0.0201 in the basal region. Ezz normal strain was higher by an average of 0.0237 and 0.00797 in the leading ($p < 0.01$) and middle regions of the cell ($p < 0.05$).

Subcellular regional strains that displayed creep behavior in both networks had their exponential time constants directly compared (Table 1). Creep was slower in the normal strains than in shear strain, as evidenced by the higher time constants to reach
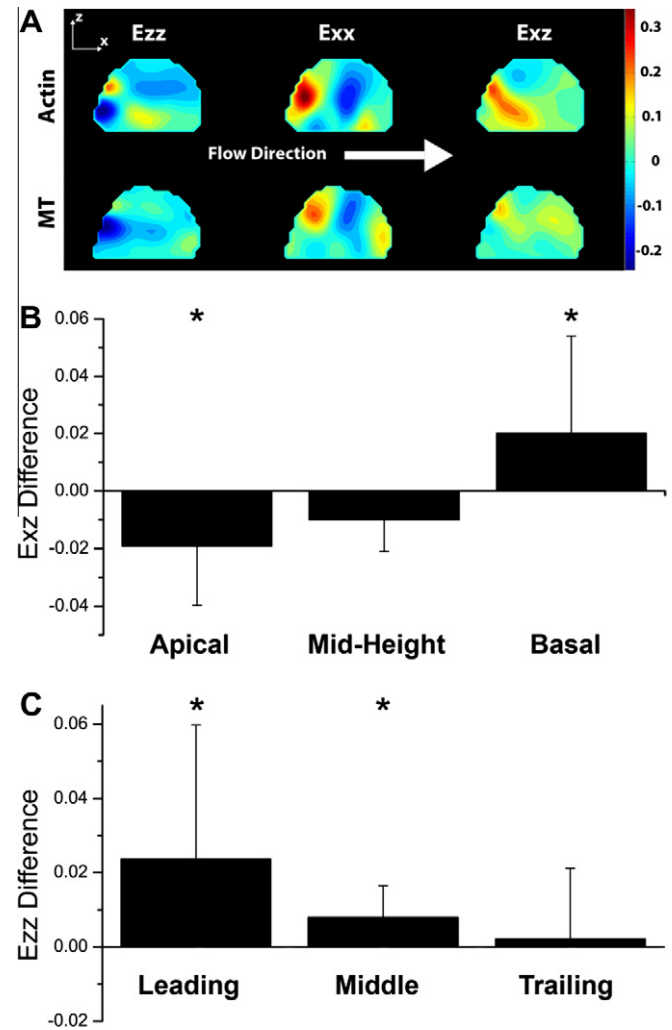
Fig. 3. (A) Strain contour plot of steady flow strains at the end of the loading period. The side-view strains of the actin and MT networks are presented from the same cell. Between the networks, the magnitudes of strains are different, and areas of tension and compression do not coincide in all areas, such as in Ezz in this cell. (B) Mean of the paired differences within each cell between the Actin and MT Exz strains at different locations in the cell at the end of the steady flow loading period. In the apical region of the cell, Actin Exz was significantly lower than MT Exz ($p < 0.01$). In the basal region of the cell, the Actin Exz was significantly greater than MT Exz ($p < 0.05$). (C) Mean of the paired differences within each cell between the Actin and MT Ezz strains at different locations in the cell at the end of the steady flow loading period. In the leading ($p = 0.05$) and middle ($p < 0.05$) regions of the cell, Actin Ezz was significantly higher than MT Ezz when comparing the paired differences between the two strains within each cell. Error bars represent standard deviation.

Table 1
Creep and creep recovery time constants for each network for the side-view strains.

Strain	Creep time constant		Creep recovery time constant	
	Actin	MT	Actin	MT
Ezz	10.67 ± 13.68^b	13.17 ± 10.12^b	2.83 ± 1.64^b	2.58 ± 1.16^b
Exx, side-view	9.60 ± 7.74^b	6.74 ± 5.66^b	$1.76 \pm 1.14^{a,b}$	$2.31 \pm 0.68^{a,b}$
Shear Exz	4.45 ± 2.83	3.77 ± 1.54	3.58 ± 1.74	3.82 ± 1.33

[a] Significantly different from other network ($p < 0.05$).
[b] Significantly different between creep and recovery ($p < 0.05$).
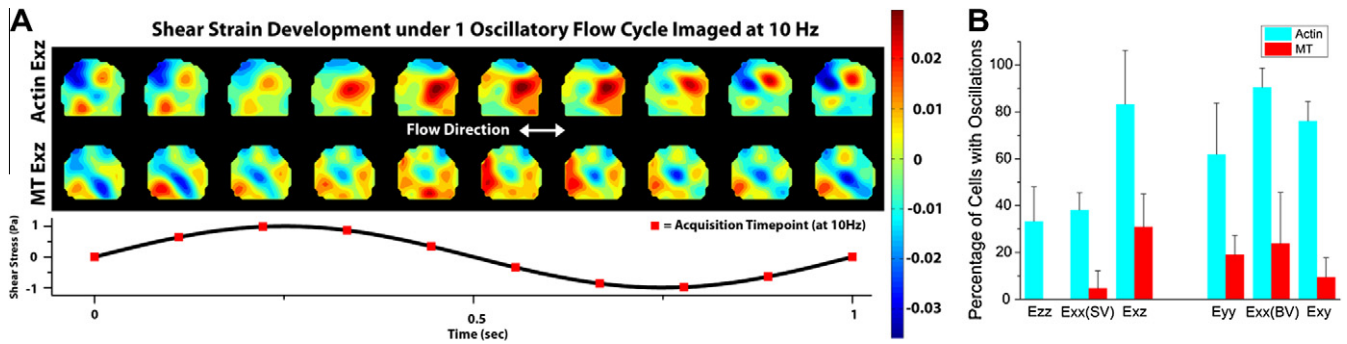
Fig. 4. (A) Actin and MT strain contour plots of the 5th cycle (of 10 total at 1 Hz) of oscillatory flow. Ten images were taken during each cycle and are presented. Strains oscillate in magnitude following the oscillatory loading profile. The areas of oscillating strains in the two networks are distinct. (B) Percentage of cells that displayed oscillatory behavior in each strain. Oscillatory strain behavior was readily apparent in the actin strains and in shear Exz. The percentages in the MT networks were always lower than in the actin networks. Error bars represent standard deviation.

equilibrium. Ezz and side-view Exx strains, but not Exz, reached equilibrium in creep recovery faster than in creep ($p < 0.05$). Creep recovery of side-view Exx, actin networks were able to reach equilibrium faster than MT networks ($p < 0.05$).

3.3. Oscillatory flow strain comparisons

The actin and MT networks had elastic-like behavior under oscillatory flow. Both networks had smaller strains than in steady flow, with heterogeneous strain patterns that oscillated with the loading profile (Fig. 4A). No residual strains were apparent after the end of flow (Fig. 2B).

Oscillations were more prevalent in the actin networks than in the MT networks (Fig. 4B). For Exz, oscillations occurred in 83.3% of the subcellular regions of the actin networks, but only in 30.9% of the subcellular regions in the MT networks. For the side-view normal strains (Ezz and side-view Exx), actin networks displayed oscillations in 35.7% of the subcellular regions, but in only 2.4% of the subcellular regions in the MT networks. However, oscillations in bottom-view normal strains (Eyy and bottom-view Exx) were more readily visible in both networks; actin and MT network bottom-view normal strains displayed oscillations in 76.2% and 21.4% of the subcellular regions, respectively.

When comparing shear Exz at the whole cell average level of cells that displayed oscillations in both networks, the average peak-to-trough amplitudes of the actin and MT networks were 0.94 ± 0.38 and 0.51 ± 0.25 (%), respectively, and the peak-to-trough amplitude was consistently higher in the actin networks than in the MT networks ($p < 0.05$).

4. Discussion

In this study, a multichannel quasi-3D microscopy technique was implemented to directly compare the fluid shear-induced strains of the actin and MT networks within a cell. Steady and oscillatory flow patterns were used to analyze differences between the two flow patterns on the cytoskeletal networks. The advantage of the multichannel quasi-3D microscopy technique was in its ability to image the two cytoskeletal networks at a sufficiently high spatiotemporal resolution to map the intracellular strains under the dynamic oscillatory fluid flow profile. Dual labeling of the actin and MT cytoskeletons has been used in studies in other cell types [24,25], but this study used a truly simultaneous, rather than sequential, acquisition of the networks. Imaging a sinusoidal loading profile without undersampling generally requires at least 6 acquisition frames per period [26]. Here, we obtained full coverage of the 1 Hz loading frequency by imaging both cytoskeletal networks at 10 Hz. Heterogeneity at the single-cell level has been ob-

served in many cytoskeletal and mechanical behavior studies [5,27,28], and this study observed that mechanical responses between the two networks were not always coupled spatially or temporally. Inter- and intracellular variability was high in this study, but the ability to pair the comparisons revealed novel observations.

Both steady and oscillatory flow produced measurable responses in shear strain Exz. Under steady flow, shear strain in both networks displayed viscoelastic behavior, while creep and creep recovery were prevalent in both networks. The differences in actin and MT peak strains may be partially explained by the spatially heterogeneous distributions of the two networks. The cortical actin networks next to the leading edge membrane experience fluid shear flow before the MT networks, as the bulk of the MT networks are more intracellular and further away from the membrane, and this shielding may explain the observed higher actin Ezz strains near the leading edge of flow. The higher observed shear Exz in the basal actin Exz may also be due to anchoring of actin at the focal adhesions at the cell-extracellular matrix interface, which the MT networks are not strongly coupled to.

The decrease in time constant between the creep from fluid shear loading and creep recovery from flow removal of both networks suggests an active cellular process that may be modulating the viscoelastic behavior of the cell and its cytoskeleton. Previous studies have demonstrated rapid reorganization of the cytoskeleton in response to flow [29], and molecular motors like myosin have been shown to be able to actively control cytoskeletal network viscoelasticity by allowing entangled cytoskeletal fibers to move more easily [30].

Under oscillatory flow, shear strain in both networks behaved elastically and followed the oscillatory loading pattern with no residual strains post-flow. The actin networks were the most responsive networks in frequency and magnitude of shear strains, suggesting that actin is an important link in mechanotransduction this physiologically relevant load level and pattern. The activation of actin-related signaling pathways but not MT-related pathways may be the link between the observed differences in steady and oscillatory flow in bone cells [13,19,31], as the MT networks are less responsive in oscillatory flow but similar in steady flow. Strain oscillations were more visible in bottom-view than side-view, emphasizing the 3D nature of the deformation. Neither view alone was sufficient to characterize the full behavior of osteocyte cell bodies under the two fluid flow profiles used in this study.

Dendritic processes have been hypothesized as mechanosensitive compartments in osteocytes [32,33]. Additional theoretical studies have mapped out the strain on the cytoskeleton in osteocyte processes in bone canaliculi [34]. The osteocyte cell body, situated in the bone lacunae, has been regarded as insensitive because it would experience lower strains *in vivo*. Recent *in vitro* and *in vivo* evidence have renewed interest in the role of the oste-

ocyte cell body in mechanotransduction. For example, focal adhesions in the osteocyte cell body *in vivo* rearrange within the cell body depending on its mechanical environment, suggesting the cell body actively senses deformation and adapts to the loading [35]. When osteocytes were not allowed to spread to avoid non-*in vivo* artifacts such as thick, aligned stress fiber formation and nuclear flattening, elastic modulus decreased and mechanosensitivity increased [10]. *In vitro* experiments that recapitulate the *in vivo* shape and organization of osteocytes may prove crucial to understanding the interplay between the osteocyte processes and the osteocyte body.

In conclusion, we have developed a novel multi-channel quasi-3D technique to measure actin and MT network strains in a single cell. Mapping the link between flow stresses and biological signaling pathway activation requires an understanding of the mechanical responses of the cellular structures, including the cytoskeleton, membrane, and nucleus. Further studies in the downstream effects of actin network deformations and its spatial heterogeneity will help elucidate these questions.

Acknowledgments

References

[1] S. Tatsumi, K. Ishii, N. Amizuka, M. Li, T. Kobayashi, K. Kohno, M. Ito, S. Takeshita, K. Ikeda, Targeted ablation of osteocytes induces osteoporosis with defective mechanotransduction, Cell Metab. 5 (2007) 464–475.

[2] S. Weinbaum, S.C. Cowin, Y. Zeng, A model for the excitation of osteocytes by mechanical loading-induced bone fluid shear stresses, J. Biomech. 27 (1994) 339–360.

[3] E.H. Burger, J. Klein-Nulend, Mechanotransduction in bone–role of the lacuno-canalicular network., FASEB J. 13 (1999) S101–S112.

[4] A.L. Rath, L.F. Bonewald, J. Ling, J.X. Jiang, M.E. Van Dyke, D.P. Nicolella, Correlation of cell strain in single osteocytes with intracellular calcium, but not intracellular nitric oxide, in response to fluid flow, J. Biomech. 43 (2010) 1560–1564.

[5] A.D. Baik, X.L. Lu, J. Qiu, B. Huo, E.M. Hillman, C. Dong, X.E. Guo, Quasi-3D cytoskeletal dynamics of osteocytes under fluid flow, Biophys. J. 99 (2010) 2812–2820.

[6] R.Y. Kwon, C.R. Jacobs, Time-dependent deformations in bone cells exposed to fluid flow *in vitro*: investigating the role of cellular deformation in fluid flow-induced signaling, J. Biomech. 40 (2007) 3162–3168.

[7] L.F. Bonewald, M.L. Johnson, Osteocytes, mechanosensing and Wnt signaling, Bone 42 (2008) 606–615.

[8] A. Vatsa, R.G. Breuls, C.M. Semeins, P.L. Salmon, T.H. Smit, J. Klein-Nulend, Osteocyte morphology in fibula and calvaria–is there a role for mechanosensing?, Bone 43 (2008) 452–458

[9] R.P. van Hove, P.A. Nolte, A. Vatsa, C.M. Semeins, P.L. Salmon, T.H. Smit, J. Klein-Nulend, Osteocyte morphology in human tibiae of different bone pathologies with different bone mineral density––is there a role for mechanosensing?, Bone 45 (2009) 321–329

[10] R.G. Bacabac, D. Mizuno, C.F. Schmidt, F.C. MacKintosh, J.J. Van Loon, J. Klein-Nulend, T.H. Smit, Round versus flat: bone cell morphology, elasticity, and mechanosensing, J. Biomech. 41 (2008) 1590–1598.

[11] K. Tanaka-Kamioka, H. Kamioka, H. Ris, S.S. Lim, Osteocyte shape is dependent on actin filaments and osteocyte processes are unique actin-rich projections, J. Bone Miner. Res. 13 (1998) 1555–1568.

[12] S.A. Murshid, H. Kamioka, Y. Ishihara, R. Ando, Y. Sugawara, T. Takano-Yamamoto, Actin and microtubule cytoskeletons of the processes of 3D-cultured MC3T3-E1 cells and osteocytes, J. Bone Miner. Metab. 25 (2007) 151–158.

[13] S.M. Ponik, J.W. Triplett, F.M. Pavalko, Osteoblasts and osteocytes respond differently to oscillatory and unidirectional fluid flow profiles, J. Cell. Biochem. 100 (2007) 794–807.

[14] X.L. Lu, B. Huo, M. Park, X.E. Guo, Calcium response in osteocytic networks under steady and oscillating fluid flow, Bone 51 (2012) 466–473.

[15] V. Pelletier, N. Gal, P. Fournier, M.L. Kilfoil, Microrheology of microtubule solutions and actin-microtubule composite networks, Phys. Rev. Lett. 102 (2009) 188303.

[16] Y.C. Lin, G.H. Koenderink, F.C. MacKintosh, D.A. Weitz, Viscoelastic properties of microtubule networks, Macromolecules 40 (2007) 7714–7720.

[17] J. Riedl, A.H. Crevenna, K. Kessenbrock, J.H. Yu, D. Neukirchen, M. Bista, F. Bradke, D. Jenne, T.A. Holak, Z. Werb, M. Sixt, R. Wedlich-Soldner, Lifeact: a versatile marker to visualize F-actin, Nat. Methods 5 (2008) 605–607.

[18] K. Faire, C.M. Waterman-Storer, D. Gruber, D. Masson, E.D. Salmon, J.C. Bulinski, E-MAP-115 (ensconsin) associates dynamically with microtubules *in vivo* and is not a physiological modulator of microtubule dynamics, J. Cell Sci. 112 (Pt 23) (1999) 4243–4255.

[19] C.R. Jacobs, C.E. Yellowley, B.R. Davis, Z. Zhou, J.M. Cimbala, H.J. Donahue, Differential effect of steady versus oscillating flow on bone cells, J. Biomech. 31 (1998) 969–976.

[20] M.A. Sutton, M.Q. Cheng, W.H. Peters, Y.J. Chao, S.R. Mcneill, Application of an optimized digital correlation method to planar deformation analysis, Image Vision Comput. 4 (1986) 143–150.

[21] J. Qiu, A.D. Baik, X.L. Lu, E.M. Hillman, Z. Zhuang, X.E. Guo, Theoretical analysis of novel quasi-3D microscopy of cell deformation, Cell Mol. Bioeng. 5 (2011) 165–172.

[22] B. Pan, H.M. Xie, Z.Q. Guo, T. Hua, Full-field strain measurement using a two-dimensional Savitzky–Golay digital differentiator in digital image correlation, Opt. Eng. 46 (2007).

[23] C.C. Wang, J.M. Deng, G.A. Ateshian, C.T. Hung, An automated approach for direct measurement of two-dimensional strain distributions within articular cartilage under unconfined compression, J. Biomech. Eng. 124 (2002) 557–567.

[24] A. Sampathkumar, J.J. Lindeboom, S. Debolt, R. Gutierrez, D.W. Ehrhardt, T. Ketelaar, S. Persson, Live cell imaging reveals structural associations between the actin and microtubule cytoskeleton in arabidopsis, Plant Cell 23 (2011) 2302–2313.

[25] W.C. Salmon, M.C. Adams, C.M. Waterman-Storer, Dual-wavelength fluorescent speckle microscopy reveals coupling of microtubule and actin movements in migrating cells, J. Cell Biol. 158 (2002) 31–37.

[26] N. Wang, S. Hu, J.P. Butler, Imaging stress propagation in the cytoplasm of a living cell, Methods Cell Biol. 83 (2007) 179–198.

[27] M.J. Jaasma, W.M. Jackson, T.M. Keaveny, The effects of morphology, confluency, and phenotype on whole-cell mechanical behavior, Ann. Biomed. Eng. 34 (2006) 759–768.

[28] J.H. Dangaria, P.J. Butler, Macrorheology and adaptive microrheology of endothelial cells subjected to fluid shear stress, Am. J. Physiol., Cell Physiol. 293 (2007) C1568–C1575.

[29] C.K. Choi, B.P. Helmke, Short-term shear stress induces rapid actin dynamics in living endothelial cells, Mol. Cell. Biomech. 5 (2008) 247–258.

[30] D. Humphrey, C. Duggan, D. Saha, D. Smith, J. Kas, Active fluidization of polymer networks through molecular motors, Nature 416 (2002) 413–416.

[31] N. Case, B. Sen, J.A. Thomas, M. Styner, Z. Xie, C.R. Jacobs, J. Rubin, Steady and oscillatory fluid flows produce a similar osteogenic phenotype, Calcif. Tissue Int. 88 (2011) 189–197.

[32] S. Burra, D.P. Nicolella, W.L. Francis, C.J. Freitas, N.J. Mueschke, K. Poole, J.X. Jiang, Dendritic processes of osteocytes are mechanotransducers that induce the opening of hemichannels, Proc. Natl. Acad. Sci. USA 107 (2010) 13648–13653.

[33] T. Adachi, Y. Aonuma, M. Tanaka, M. Hojo, T. Takano-Yamamoto, H. Kamioka, Calcium response in single osteocytes to locally applied mechanical stimulus: differences in cell process and cell body, J. Biomech. 42 (2009) 1989–1995.

[34] Y. Wang, L.M. McNamara, M.B. Schaffler, S. Weinbaum, A model for the role of integrins in flow induced mechanotransduction in osteocytes, Proc. Natl. Acad. Sci. USA 104 (2007) 15941–15946.

[35] A. Vatsa, C.M. Semeins, T.H. Smit, J. Klein-Nulend, Paxillin localisation in osteocytes––is it determined by the direction of loading?, Biochem Biophys. Res. Commun. 377 (2008) 1019–1024.